Physical Modelling in Geotechnics – McNamara et al. (Eds)
© 2018 Taylor & Francis Group, London, ISBN 978-1-138-34422-8

Model tests on soil displacement effects for differently shaped piles

A.A. Ganiyu
Department of Civil Engineering and Quantity Surveying, Military Technological College, Muscat, Oman

A.S.A. Rashid & M.H. Osman
Faculty of Civil Engineering, Universiti Teknologi Malaysia, Skudai, Johor, Malaysia

W.O. Ajagbe
Department of Civil Engineering, Faculty of Technology, University of Ibadan, Ibadan, Nigeria

ABSTRACT: Transparent synthetic soil synthetic soil surrogates which permit real-time visualisation of soil continuum during testing is a novel development for geotechnical physical model tests. This paper presents model tests on pile penetration effects of differently shaped model piles subjected to axial loads in transparent synthetic soil model. Model piles, made of mortar of square, hexagonal, octagonal and circular shapes were utilised for the research. The transparent soil was made from fumed silica powder and pore fluid containing Paraffin and Technical White Oil. Soil displacement patterns were captured non-intrusively using close range photogrammetry while Particle Image Velocimetry (PIV) was employed to analyse the images. The analysed results revealed that the displacements of soil beneath the square pile aligned perfectly vertical with the edge of the pile, while it inclined with the vertical for piles of other shapes; this angle of inclination θ also varies for the variously shaped piles. This result, which depicts varying displacement patterns of soils beneath the differently shaped piles and marks distinguishable features for each shape of pile is significant. It could be used as the basis for the evolution of design charts and protocols based on shape of piles.

1 INTRODUCTION

Transparent synthetic soil surrogates which permit real-time visualisation of soil continuum during testing is a novel development to geotechnical physical model tests (Ganiyu et al., 2016, Kong et al., 2018, Xiao et al., 2017). Transparent soil is produced from synthetic aggregates and pore fluids with matching refractive indices, thus permitting complete penetration of light (Iskander et al., 2015, Kong et al., 2017). Transparent soil is an effective tool for modelling soil-structure interaction mechanisms; and its incorporation with Particle Image Velocimetry (PIV) provides an innovative technique for the visualization of failure mechanisms and the quantification of soil–structure interaction problems in geotechnical physical models non-intrusively (Omidvar and Iskander, 2017, Xiao et al., 2016, Yin et al., 2017).

PIV is an image-processing technology that computes fields of incremental displacement by comparing two successive images through a precise identification of several minute parts in image space (pixel) which are later converted to object space (in millimetres) (Take, 2015, Sui and Zheng, 2017, Rashid et al., 2017). GeoPIV is a MATLAB based PIV module developed specifically for geotechnical applications. In GeoPIV, image processing algorithms are written to apply the PIV principle to the images of soil (Stanier et al., 2015, Chen et al., 2016, Rashid et al., 2014). Internal displacements and deformations in a transparent soil slurry are measured by relating images of speckles that are generated both before and after soil deformation. This is obtained by employing GeoPIV combined with advance photogrammetry and the use of laser light source to optically slice the soil (Ganiyu, 2016, Qi et al., 2016).

The study of soil movement beneath a pile during installation is highly essential. The repositioning of soil beneath a pile subjected to dynamic forces may impact underground services such as tunnels and pipelines, adjacent foundations or archaeological remains (Hird et al., 2011). Furthermore, the design of pile foundation is mostly a function of the applied load and the resisting capacity of pile. The resistance of the pile is influenced by the state and properties of soils within the critical zone immediately surrounding the pile (Burland, 2012, Tomlinson and Woodward, 2014).

Precast concrete piles are prefabricated, displacement piles of different solid cross sections. However, little is known about the effect of the different shapes of piles when they interact with the adjoining soils. Many design equations and charts in geotechnical engineering were developed based on failure planes measured from physical model tests (Iskander and Liu,

Figure 1. Piles cast with pipes at top.

2010). The goal of this paper is to advance the understanding of soil-pile interaction for differently shaped piles through the investigation of displacement of soil underneath the piles using transparent synthetic soil and PIV.

2 MATERIAL AND TESTING

2.1 *Model piles*

The model piles were cast with mortar in the laboratory. The cement was Ordinary Portland Cement (OPC) while the fine aggregate was naturally occurring river sand; a mix ratio of 1:3 for cement: sand; and a water: cement (w/c) ratio of 0.45 was used to make the mortar. Four model piles of circular, square, hexagonal and octagonal shapes with overall cross sectional area of 452.4 mm^2 and length 100 mm were cast. The circular pile is 24 mm in diameter, while the length of side of the square, hexagonal and octagonal piles are 21.27, 13.2 and 9.68 mm respectively. During casting 8 mm diameter circular plastic pipes were inserted to a depth of 10 mm at the top centre of each pile, Figure 1 shows the pile cast with pipes at top centre.

The castings were demoulded after 24 hours and cured in water for 28 days. The average value of the compressive strength of the mortar cubes cast along with the model piles was 38.0 MPa. The inserted pipes were removed after the curing process; and the removal of these pipes created a hole of 8 mm diameter and 10 mm deep at the top centre of each of the piles. The holes later served as the point of insertion for the connector during penetration tests. The piles have a smooth surface finish and the surfaces were later sprayed with black Aerosol spray paint to ensure that the piles have the required black background necessary for laser light during penetration tests (Sills et al., 2017).

2.2 *Transparent synthetic soil*

Transparent synthetic soil was made from Fumed Silica powder (HDK–N20) as the aggregate component, while Technical White Oil ISO 15 (Grade A) and Paraffin oil (P1000) form the pore fluid. A ratio of 23% Paraffin and 77% technical white oil was adopted for the pore fluids (Stanier et al., 2014); while the aggregate was 5% of the total mass of the transparent soil. This mix gave the best quality of transparency after a series of trial mixes. Specifically, 850 g of technical white oil was mixed with 254 g of paraffin oil to form the pore fluid. Also, 0.012 g of Timiron Ultraluster MP-111 powder was added to the pore fluid to provide the contrast (texture) (Hird and Stanier, 2010). The mixture was then added to 58.2 g of fumed silica and an intense mixing was carried out using the whisk until a completely homogeneous mix was formed. The mass of Timiron represents 0.02% of the aggregate mass (Stanier et al., 2012).

The slurry formed was yet to be transparent as it contained a significant amount of air. Due to this, a vacuuming process was performed to de-air the slurry. The slurry was poured into a cylindrical chamber of diameter 90 mm and height 260 mm, made from Perspex and connected to a vacuum pump. The vacuum pump was switched on and the de-airing process took place for six hours (Iskander et al., 2002). Thereafter, testing cylinder containing the transparent soil was coupled to the consolidation frame. The arrangement was left for 24 hours and it ensures consolidation under self-weight of the transparent soil. Successive increasing load of 3.125, 6.25, 12.5, 25, 50 and 100 kPa was added and each load was maintained for a period of 24 hours (Hakhamaneshi and Black, 2016). After the peak load of 100 kPa, the loading was reduced to 50 kPa and maintained for another 24 hours. This gives an overconsolidation ratio of 2. The height of the sample was recorded before the consolidation began, prior to adding successive loadings and at the end of the consolidation test. Figure 2 shows the full arrangement of the consolidation process.

2.3 *Penetration tests*

After the consolidation was achieved, the set-up was decoupled again and the target markers were carefully gummed to the surface of the testing cylinder to serve as control points for the imminent penetration test. Target markers were made as stationary control points because they were needed in the image to permit a distinction between the soil and camera movements (Kelly and Black, 2012). Two columns of the target markers were spaced at 20 mm centre to centre on vertical axis, and the columns spaced at 50 mm centres.

The testing cylinder was placed directly underneath the driving unit. A driving unit that generates a constant rate of penetration of the model pile into the soil was provided for the loading test. The rate of drive unit penetration was 50 mm/minute as obtained in the calibration test. The LVDT was connected to the top, while the load cell was mounted at the lower end connected

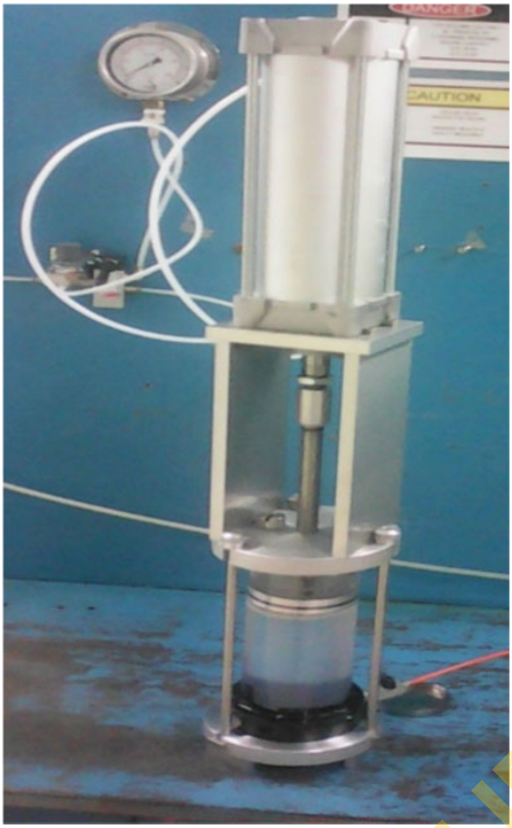

Figure 2. Transparent soil under consolidation.

to a flat tipped adaptor. Meanwhile, the adaptor has been rigidly joined with the black painted model pile via the hole at its top, with the help of gap sealant. The driving unit was carefully lowered until the base of the model pile was at the surface of the transparent soil.

Afterwards, a green diode-pumped solid-state (DPSS) laser apparatus was connected to power source and placed on the left side of the testing chamber. The laser head was adjusted until its illuminated vertical section aligned with the centreline of the pile and focused on the area directly beneath the pile. The interaction between the transparent soil and the laser light produced a distinctive laser speckle pattern. A Nikon D5100 digital camera was mounted on its tripod base and placed in front of the testing chamber; 300 mm away, and carefully set to focus the test arrangement, particularly the interface of the model pile and the transparent soil. A spirit level was used to confirm the correctness of both the vertical and horizontal alignments of the camera, and a remote control was connected to the camera. Figure 3 shows the set-up for the penetration test.

The actual penetration test was carried out in a 'dark room' situation (Qi et al., 2016, Black and Tatari, 2015). The driving unit was released to facilitate the downward movement of the pile with a simultaneous activation of the camera. The images were captured in a continuous shooting mode at an average rate of 0.8 frame per second. The values of the loads and displacements of the pile during the penetration test were recorded by the logging system. The test was terminated when the penetration of the pile reached 20 mm. The procedure was repeated for the remaining three piles of other shapes. Figure 4 shows the progressive downward movement of pile with example images taken at different times during a penetration test.

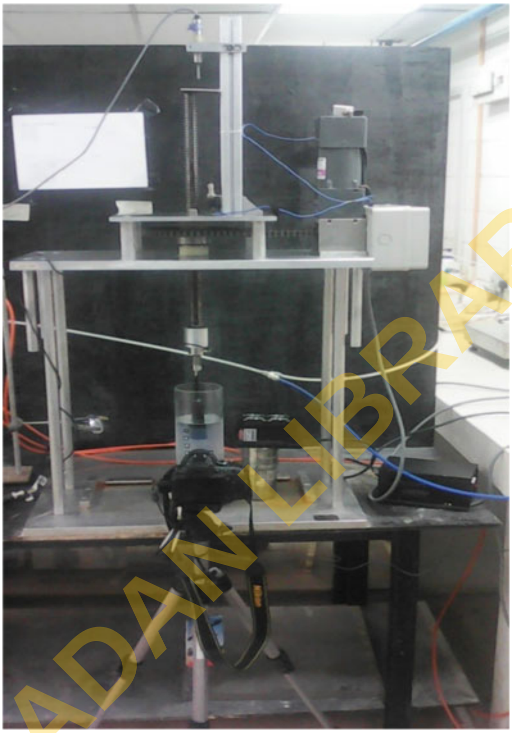

Figure 3. Set-up for the pile penetration test.

2.4 *PIV analysis*

The images from the penetration tests were downloaded from the camera to the computer. A total of 100 images were selected for analysis for each test; the images adequately cover the penetration process from the beginning to a convenient point proximate to the termination of each tests. GeoPIV8, a Matlab based PIV module developed by (White and Take, 2002) was employed for the analysis of the images.

3 RESULTS AND DISCUSSION

3.1 *Consolidation properties of transparent soil*

Figure 5 shows the time-settlement graph for the consolidation for 0 to 100 kPa for the square pile, and this is typical for all the four tests as the values closely matched one another. The steep slope between the first

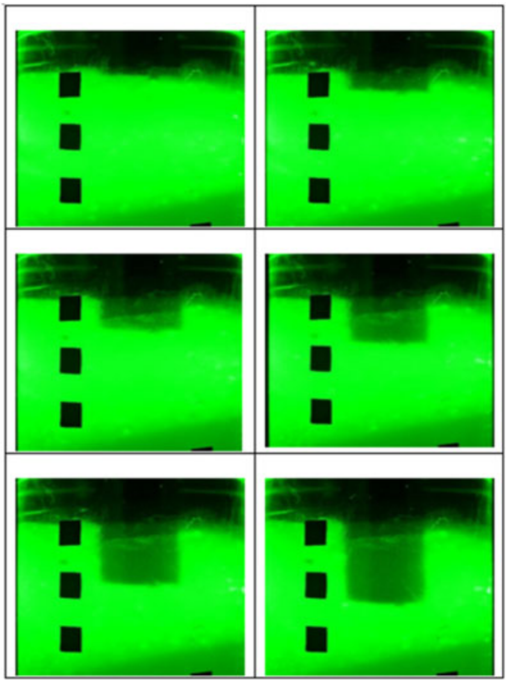

Figure 4. Progressive downward movement of pile during the penetration test.

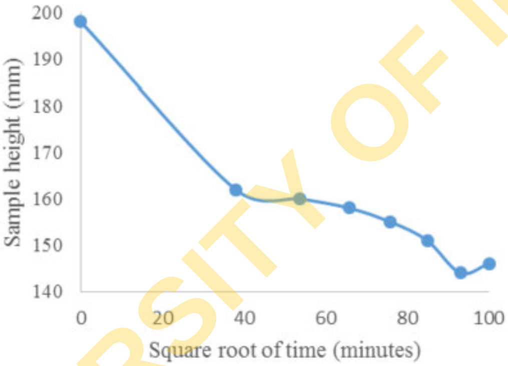

Figure 5. Consolidation plot for transparent soil.

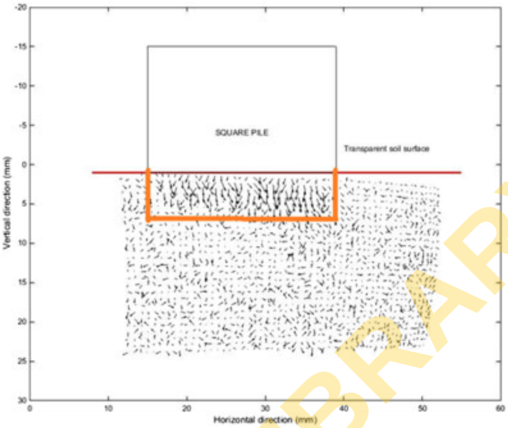

Figure 6. Displacement beneath square pile.

two points is as a result of the consolidation under self-weight of the freshly prepared transparent soil. There is rapid release of pore fluid during this period; which is the first 24 hours after the soil was prepared, due to agglomeration of the aggregate components.

The coefficient of consolidation c_v was derived by using the Taylor's method for the loading range between 3.125–100 kPa. The coefficient of consolidation, c_v obtained was 0.965 m^2/year. This value of c_v falls within (0.9 ± 0.2) reported by (Lehane and Gill, 2004) and (0.8–1.2) reported by (McKelvey et al., 2004) and (Sivakumar et al., 2007). The coefficient of compressibility, m_v and the hydraulic conductivity, k were obtained as 1.15 m^2/MN and 2.93×10^{-9} m/s respectively. (McKelvey et al., 2004) reported similar coefficients of compressibility, m_v values while the hydraulic conductivity, k value is also within the range of values reported by (Lehane and Gill, 2004) and (Song et al., 2009). Thus, the transparent soil prepared and employed for this research can be categorized as a normally consolidated alluvial clay.

3.2 *Pile penetration effects in transparent soil*

PIV analysis was done and terminated at the vector plots stage to show the soil movements beneath the piles; the stage shows the displacements of soils at vertical directions underneath the differently shaped piles. According to previous researches on anchors (Ilamparuthi et al., 2002, Ilamparuthi and Muthukrishnaiah, 1999), and laterally loaded piles (Liu et al., 2010), it was assumed that the failure plane from soil displacement is similar to that of the shear strain field. The failure plane was delineated beneath the piles, and it was depicted by joining the points which had clear-cut vertical displacements of half the maximum vertical displacements beneath the piles. Figures 6–9 show the soil displacements underneath the square, hexagonal, octagonal and circular piles, respectively.

From the Figures, it was observed that the displacements of soil beneath the square pile align perfectly vertical with the edge of the pile, while it inclined with the vertical for the piles of other shapes. This angle of inclination θ also varies for the variously shaped piles; θ was determined to be 45° and 49.4° for the hexagonal pile; 33.7° and 41.6° for the octagonal pile; and 36.9° and 51.3° for the circular pile, respectively. It can be deduced that the behaviour manifested by the square pile is due to the flat plane of its sides/edges; while for the other shapes, it is based on the curvilinear plane of their respective sides/edges. Hence, it is concluded that the soil movements underneath an axially loaded penetrating pile is influenced by the shape of the pile, therefore, soil – pile interaction beneath differently shaped pile under axial load will be affected by the shape of the pile.

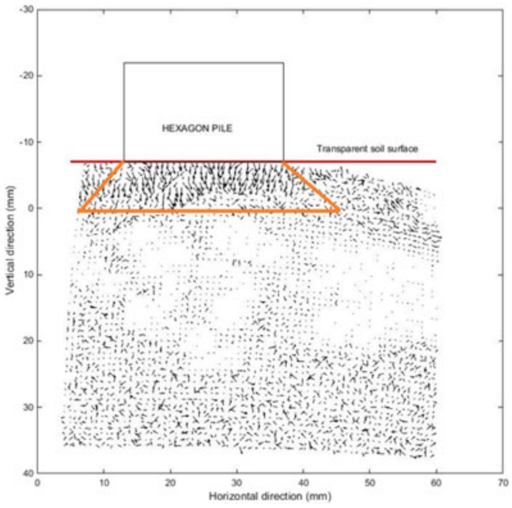

Figure 7. Displacement beneath hexagonal pile.

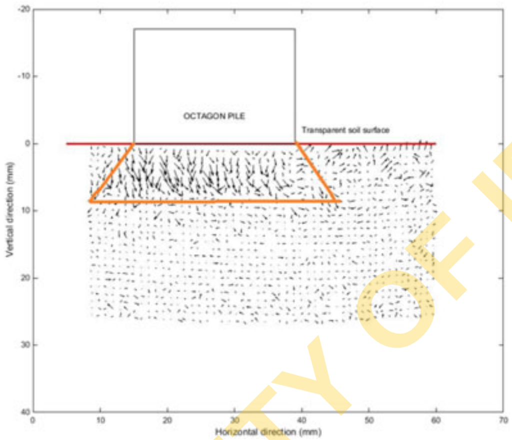

Figure 8. Displacement beneath octagonal pile.

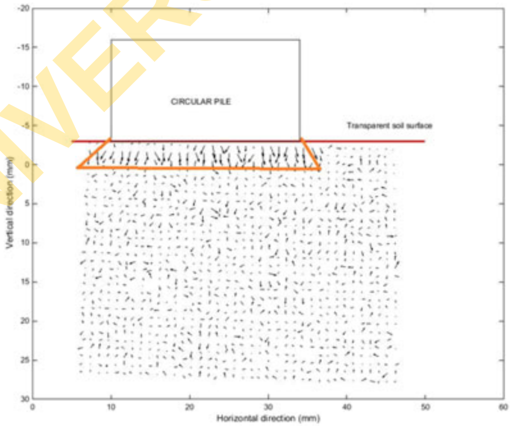

Figure 9. Displacement beneath circular pile.

4 CONCLUSIONS

Transparent soil with geotechnical properties replicating normally consolidated alluvial clay was prepared from synthetic materials. The soil enabled a real-time visualisation of the penetration of differently shaped piles installed in a unit gravity model test. In addition, the displacement effects of soil beneath the differently shaped piles were studied using close range photogrammetry while PIV was used to analyse the images taken during the penetration tests. The results revealed the differences in displacement patterns of soils beneath the differently shaped piles. It was therefore concluded that soil movements underneath an axially loaded penetrating pile can be associated with the shape of the pile. These marked distinguishable features for each shape of pile is a potential. In future, it could be the basis for the evolution of design charts and protocols based on the geometry of piles.

REFERENCES

Black, J. A. & Tatari, A. 2015. Transparent Soil to Model Thermal Processes: An Energy Pile Example. Geotechnical Testing Journal 38(5):1–13.

Burland, J. B. 2012. Behaviour of Single Piles Under Vertical Loads. In ICE Manual of Geotechnical Engineering, Institution of Civil Engineers, United Kingdom, pp. 231–246.

Chen, Z., Li, K., Omidvar, M. & Iskander, M. 2016. Guidelines for DIC in geotechnical engineering research. International Journal of Physical Modelling in Geotechnics: 1–20.

Ganiyu, A. A. 2016. Influence of Axially Loaded Shaped Pile on Geotechnical Capacity. PhD Thesis, Faculty of Civil Engineering, Universiti Teknologi Malaysia, Skudai, Johor, Malaysia.

Ganiyu, A. A., Rashid, A. S. A. & Osman, M. H. 2016. Utilisation of transparent synthetic soil surrogates in geotechnical physical models: A review. Journal of Rock Mechanics and Geotechnical Engineering 8(4):568–576.

Hakhamaneshi, M. & Black, J. A. 2016. Shear Strength of Transparent Gelita—The Effect of the Mixture Ratio, Displacement Rate, and Over-Consolidation Ratio. In Geo-Chicago 2016, pp. 443–452.

Hird, C. C., Ni, Q. & Guymer, I. 2011. Physical modelling of deformations around piling augers in clay. Géotechnique 61(11):993–999.

Hird, C. C. & Stanier, S. A. 2010. Modelling Helical Screw Piles in Clay Using a Transparent Soil. In Physical Modelling in Geotechnics, CRC Press, Zurich, Switzerland, pp. 769–774.

Ilamparuthi, K., Dickin, E. A. & Muthukrisnaiah, K. 2002. Experimental investigation of the uplift behaviour of circular plate anchors embedded in sand. Canadian Geotechnical Journal 39(3):648–664.

Ilamparuthi, K. & Muthukrishnaiah, K. 1999. Anchors in sand bed: delineation of rupture surface. Ocean Engineering 26(12):1249–1273.

Iskander, M., Bathurst, R. J. & Omidvar, M. 2015. Past, Present, and Future of Transparent Soils. Geotechnical Testing Journal 38(5):1–17.

Iskander, M. & Liu, J. Y. 2010. Spatial Deformation Measurement Using Transparent Soil. Geotechnical Testing Journal 33(4):314–321.

Iskander, M. G., Liu, J. Y. & Sadek, S. 2002. Transparent Amorphous Silica to Model Clay. Journal of Geotechnical and Geoenvironmental Engineering 128(3):262–273.

Kelly, P. & Black, J. A. 2012. Optimisation of Stone Column Design Using Transparent Soil and Particle Image Velocimetry (PIV). In ISSMGE – TC 211 International Symposium on Ground Improvement IS-GI, Brussels, Belgium, vol. III, pp. 443–452.

Kong, G., Li, H., Yang, G. & Cao, Z. 2018. Investigation on shear modulus and damping ratio of transparent soils with different pore fluids. Granular Matter 20(1).

Kong, G. Q., Li, H., Hu, Y. X., Yu, Y. X. & Xu, W. B. 2017. New Suitable Pore Fluid to Manufacture Transparent Soil. Geotechnical Testing Journal 40(4):20160163.

Lehane, B. M. & Gill, D. R. 2004. Displacement Field Induced by Penetrometer Installation in an Artificial Soil. International Journal of Physical Modelling in Geotechnics 4(1):25–36.

Liu, J., Liu, M. & Gao, H. 2010. Influence of Pile Geometry on Internal Sand Displacement around a Laterally Loaded Pile Using Transparent Soil. In GeoShangai International Conference ASCE, pp. 1–7.

Mckelvey, D., Sivakumar, V., Bell, A. & Graham, J. 2004. Modelling Vibrated Stone Columns in Soft Clay. Proceedings of the Institution of Civil Engineers-Geotechnical Engineering 157(3):137–149.

Omidvar, M. & Iskander, M. 2017. Soil Deformations during Finless Torpedo Installation. In Geotechnical Frontiers 2017, pp. 389–397.

Qi, C.-G., Iskander, M. & Omidvar, M. 2016. Soil Deformations During Casing Jacking and Extraction of Expanded-Shoe Piles, Using Model Tests. Geotechnical and Geological Engineering 35(2):809–826.

Rashid, A. S. A., Black, J. A., Mohamad, H. & Mohd Noor, N. 2014. Behavior of Weak Soils Reinforced with End-Bearing Soil-Cement Columns Formed by the Deep Mixing Method. Marine Georesources & Geotechnology 33(6):473–486.

Rashid, A. S. A., Kueh, A. B. H. & Mohamad, H. 2017. Behaviour of soft soil improved by floating soil–cement columns. International Journal of Physical Modelling in Geotechnics:1–22.

Sills, L.-a. K., Mumford, K. G. & Siemens, G. A. 2017. Quantification of Fluid Saturations in Transparent Porous Media. Vadose Zone Journal 16(2):0.

Sivakumar, V., Glynn, D., Black, J. & Mcneill, J. 2007. A Laboratory Model Study of the Performance Of Vibrated Stone Columns in Soft Clay. In 14th European Conference on Soil Mechanics and Geotechnical Engineering, Madrid, Spain, pp. 1–6.

Song, Z. H., Hu, Y. X., O'loughlin, C. & Randolph, M. F. 2009. Loss in Anchor Embedment During Plate Anchor Keying in Clay. Journal of Geotechnical and Geoenvironmental Engineering 135(10):1475–1485.

Stanier, S. A., Blaber, J., Take, W. A. & White, D. J. 2015. Improved Image-Based Deformation Measurement for Geotechnical Applications. Canadian Geotechnical Journal 53(5):727–739.

Stanier, S. A., Black, J. A. & Hird, C. C. 2012. Enhancing Accuracy and Precision of Transparent Synthetic Soil Modelling. International Journal of Physical Modelling in Geotechnics 12(4):162–175.

Stanier, S. A., Black, J. A. & Hird, C. C. 2014. Modelling Helical Screw Piles in Soft Clay and Design Implications. Proceedings of the Institution of Civil Engineers-Geotechnical Engineering 167(5):447–460.

Sui, W. & Zheng, G. 2017. An experimental investigation on slope stability under drawdown conditions using transparent soils. Bulletin of Engineering Geology and the Environment, pp. 1–9.

Take, W. A. 2015. Thirty-Sixth Canadian Geotechnical Colloquium: Advances in Visualization of Geotechnical Processes Through Digital Image Correlation. Canadian Geotechnical Journal 52(9):1199–1220.

Tomlinson, M. & Woodward, J. 2014. Pile Design and Construction Practice. 6th edn., CRC Press.

White, D. J. & Take, W. A. 2002. GeoPIV: Particle Image Velocimetry (PIV) Software for use in Geotechnical Testing, CUED/D-SOILS/TR322, University of Cambridge.

Xiao, Y., Sun, Y., Yin, F., Liu, H. & Xiang, J. 2017. Constitutive Modeling for Transparent Granular Soils. International Journal of Geomechanics 17(7):04016150.

Xiao, Y., Yin, F., Liu, H., Chu, J. & Zhang, W. 2016. Model Tests on Soil Movement during the Installation of Piles in Transparent Granular Soil. International Journal of Geomechanics, 17(4), pp. 06016027-1/7

Yin, F., Xiao, Y., Liu, H., Zhou, H. & Chu, J. 2017. Experimental Investigation on the Movement of Soil and Piles in Transparent Granular Soils. Geotechnical and Geological Engineering, pp. 1–9.